VANCE PRESS

Rock Mechanics Letters

www.journal-rml.com

Research Article

The Conundrum of the Crack Initiation Stress of Rock Type Material – I. The Trapezoid Rule Method

Dimitrios Papadomarkakis[1,*]

[1] *Laboratory of Tunneling, School of Mining and Metallurgical Engineering, National Technical University of Athens, Zografou Campus, Athens, Greece*
[*] Correspondence: papadomarkakisdimitrios@gmail.com

Received: 17 July 2025
Revised: 24 July 2025
Accepted: 28 July 2025
Published date: 3 August 2025
Doi: 10.70425/rml.202503.20

Abstract: In part I of this study, the great practical importance of the onset of stable crack growth was outlined, since several researchers have supported that it can serve as a more realistic estimation of the in-situ spalling strength of the rock mass, in comparison with the more frequently used uniaxial compressive strength. Moreover, a short review was also provided regarding the empirical techniques that have been proposed in the last six decades for the prediction of the crack initiation stress. The main criticism of each method was also mentioned. Subsequently, a new method was proposed, based on the Trapezoid Rule, an elementary calculus approximation technique. The latter technique possesses a strong and robust physical explanation, easy application, and complete objectiveness. The Trapezoid Rule method was applied to ten rock specimens, eight marbles and two vesicular basalts, that were subjected to uniaxial compressive tests. The results of the newly suggested method were compared to those obtained using the established methods of the existing literature. Ultimately, it displayed exceptionally close results with all other methods for the ten specimens, thus indicating that it can accurately and consistently predict the crack initiation stress for the two rock types. In future research efforts, the proposed technique should be applied to a wider range of rock types, such as granites, andesites, limestones, to investigate its general applicability.

Keywords: Crack initiation; Crack damage; Uniaxial compressive tests; Brittle fracture

1. Introduction

The fracturing process, as well as fracture mechanics, of rocks is of great importance to underground works and excavations, because it can help engineers and geologists gain insights into the behavior of the surrounding rock mass, and especially the overburden strata. It is generally accepted that rocks experience a very sudden form of failure which usually occurs shortly after plastic deformation commences, this type of failure is often referred to as brittle failure. The brittle fracture pathway of rock-type material has been investigated by researchers for almost 60 years (e.g. [1–14]). Although many questions still remain unanswered it has generally been accepted amongst researchers that the brittle failure of low porosity rocks can be divided by four distinct stages, with each stage accounting for a different deformation stage phase of the rock.

The aforementioned stages were first observed in the studies of Brace et al. [1] and Bieniawski [2], with the latter subjecting a granite, a marble, and an applite to triaxial compressive tests, while the last utilized uniaxial, biaxial, and triaxial compressive loading conditions on norite and quartzite specimens. Consequently, these stages were recognised by the different responses of the stress-strain curves which were obtained from the respective compressive tests of each rock sample. Namely, the four stages which were documented were: (1) the Crack Closure (CC) stage, (2) the Crack Initiation (CI) phase, (3) the Crack Damage (CD) stage, and finally the peak strength of the rock [5-9,11-14]. As it can be seen in Figure 1, each deformation stage is separated by an important stress threshold, specifically stage (1) ends when the CC stress is reached which subsequently marks a linear response of the axial stress-axial strain curve. During this phase pre-existing cracks are compressed and subsequently closed. However, if the rock sample contains a significant volume of pre-existing cracks (or showcases increased porosity, meaning great volume of voids) it has been well documented that this stage may be completely absent [5,6]. Moreover, stage (2) ends when the CI stress is reached which coincides with the onset of stable crack growth within the rock. It is worth noting that this point corresponds to the stress threshold where the axial stress-lateral strain (or the axial stress-volumetric strain) curve departs from linearity. Furthermore, stage (3) concludes when the CD stress is obtained, meaning when unstable crack propagation begins. This point corresponds to the reversal point of the axial stress-volumetric strain curve or simply the maximum volumetric strain value. Finally, stage (4) ends when the peak compressive strength of the rock is achieved.

The accurate prediction of the CI stress of rock-type material has been a topic of hot debate amongst researchers for many years (e.g. [5-9,11-14]), due to its high significance in deep underground mining and tunnelling projects, where major spalling failure has been observed in the surrounding rock mass [7]. Fairhurst and Cook [15] were one of the first to study the spalling that was noticed around some deep South African tunnels by essentially extending the Griffith cracks for a compressive stress field, which lengthens parallel to the maximum compressive stress. Almost 15 years later, Hoek and Brown [16] came to the conclusion that after the exerted stress surpasses close to 15% of the Uniaxial Compressive Strength (UCS) spalling failure begins around the underground opening. This conclusion was drawn based on observations of square tunnels in South Africa. Close to two decades later, Martin et al. [17] transformed the Hoek-Brown failure criterion into a maximum tangential stress criterion and discovered that when the maximum tangential stress exceeded a threshold of approximately 40% of the UCS, significant slabbing occurred. Furthermore, 10 years later Rojat et al. [18] utilized the aforesaid criterion and subsequently applied it to the Lötschberg tunnel, which is located in Switzerland, in an attempt to explain the many stress induced problems that were encountered with the usage of Tunnel Boring Machines at the depths greater than 1 km. From their analysis it was concluded that the in-situ spalling strength of the rock mass does not coincide with the UCS, hence using the later to predict the in-situ spalling strength during the design phase can lead to extended down times due to the overestimation of the strength. The previously mentioned studies clearly indicated that the UCS of the intact rock cannot properly determine the spalling strength of the rock mass around an underground opening. As a result, researchers recommended the CI stress as a more accurate estimation for the in-situ spalling strength [19,20].

Despite the utmost importance of the CI stress of rock-type material, to this day researchers have not collectively agreed upon a universal way for determining its threshold, thus prompting various authors to suggest different empirical techniques capable of identifying it (e.g. [1-14]). Moreover, it is worth noting that ISRM [21] did not propose a unified method for its determination [8], resulting in even further confusion as to which of the proposed techniques is more reliable and accurate.

Overall, the aim of this two-part study is to propose two new techniques for the prediction of the CI stress. These two new methods essentially determine the CI threshold using two elementary mathematical

approaches. Namely, in part I the Trapezoid Rule (TR) method is presented, while in part II the Second Derivative Method (SDM) is explained, respectively. Both of the newly suggested methods were applied to the results obtained from ten uniaxial compressive tests conducted on eight marbles specimens of low porosity and two vesicular basalts of increased porosity, in order to predict the stable crack growth threshold of the aforesaid samples. The results of the methods were then compared with those obtained by the established empirical techniques that were available in the existing literature. Hence from the simple statistical analysis that was conducted it was made clear that both newly suggested mathematical methods yielded exceptionally close results with the frequently utilized empirical techniques for the eight marble samples. Subsequently, the two new methods can predict the onset of stable crack growth correctly for the previous rock type. Additionally, the TR method had only minor differences with the other established techniques of the litterature for the two basalts. On the contrary, the SDM showcased a very poor correlation with the other methods for the same two rock samples. Consequently, more specimens of the aforementioned rock type need to be tested in the future, in order to fully comprehend if the TR and the SDM can consistently and accurately determine the CI stress for that rock type.

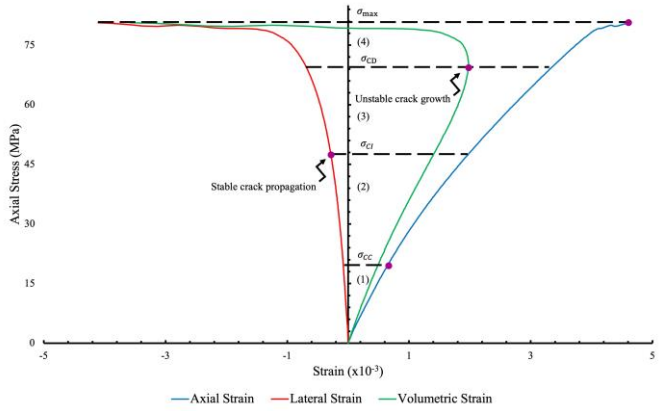

Figure 1. Typical stress-strain curves that are obtained from a uniaxial compressive test.

2. Rock Specimens

The ten rock specimens that were subjected to uniaxial compressive tests were eight marbles, and two vesicular basalts. In this section of this two-part study the dimensions, as well as the physical properties of the specimens are presented. The two vesicular basalts had a characteristic moldic type porosity (see Figure 2), according to the classification of Choquette and Pray [22]. In contrast, the eight marble specimens did not display any characteristic porosity types, since their overall porosity was negligible. Moreover, the average dry densities of the eight marbles and the two basalts were 2.80 g/cm^3 and 2.33 g/cm^3, respectively. Furthermore, the porosity of the two basaltic rocks was estimated using an image analysis technique originally proposed by Al-Harthi et al. [23]. The method essentially involved scanning the upper and lower areas of the samples as digital images, then the scanned photos were inserted in an open access image analysis software called FIJI. Using the color threshold capabilities of the latter software the images were separated into two layers, particulalry the black color vesicules (voids) were differentiated by the brighter color pixels which composed the rock frame (see Figure 3). As a result, the areas of the two aforementioned layers were calculated and consequently an estimation of the porosity of the samples was produced. The average porosity of the two samples was around 18%.

The porosity of the eight marble specimens was not calculated, because it did not have any practical importance. Lastly, in Table 1 below the dimensions, particulalry the diameters, lenghts, and height to diameter ratios, of the ten rock specimens are documented.

3. Compression Tests

The uniaxial compressive tests were executed on the Advantest 9 servo-hydraulic test machine with a maximum loading capacity of 5000 kN, following the ISRM 1999 suggested methods guidelines for the complete stress-strain curves for intact rock in uniaxial compression. As it can be seen from Figure 4, the axial displacement was measured by recording the change of axial distance between two aluminium rings that were attached close to the middle third of each specimen. The axial distance between the two rings was computed by three Linear Variable Differential Transducers (LVDTs) that were placed at an angle of approxiamtely 120° apart from each other. Thus, the total axial strain was evaluated as the average axial strain of the three LVDTs. Additionally, a circumference chain extensometer was attached at the mid-height of each specimen, in order to record circumference changes, and ultimately the lateral strain. Furthermore, the volumetric strain was calculated by the following expression:

$$\varepsilon_V = \varepsilon_a + 2\varepsilon_l \quad (1)$$

where, ε_V: denotes the volumetric strain, ε_a: represents the axial strain, and ε_l: symbolizes the lateral strain.

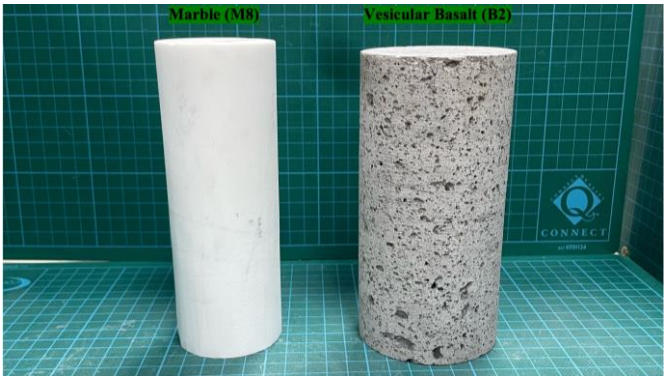

Figure 2. The two different rock types that were tested.

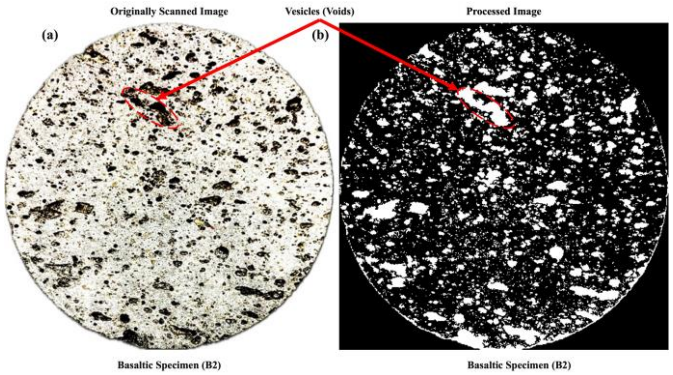

Figure 3. (a) Scanned surface of basaltic specimen B2; (b) post-processed result of the scanned image.

Table 1. The physical properties of the ten rock samples.

Rock type	Specimen designation	Dry density (g/cm^3)	Porosity (%)	Height (mm)	Diameter (mm)	Height to diameter ratio
Marble	M1	2.79	-	151.73	56.24	2.69
	M2	2.81	-	151.03	56.16	2.68
	M3	2.79	-	152.06	55.05	2.76
	M4	2.81	-	150.92	56.14	2.68
	M5	2.80	-	151.74	56.21	2.69
	M6	2.80	-	150.91	54.36	2.77
	M7	2.81	-	150.89	54.07	2.79
	M8	2.79	-	150.92	54.40	2.77
Basalt	B1	2.35	18.10	146.50	72.66	2.01
	B2	2.32	17.40	146.20	72.70	2.01

The tests of the eight marble samples, as well as that of basaltic specimen B2, were conducted using axial load control, with a loading rate of approxiamtely 0.50 MPa/sec. The compressive test of basaltic specimen B1 was conducted using lateral displacement control, with a displacemnt rate of 7 μm/min, this rate was doubled after the specimen entered the post failure region.

From these ten uniaxial compressive tests the strength, the elastic constants, i.e. Young's modulus and Poisson's ratio, and the stress-strain curves for each rock specimen were obtained. In Table 2 below the aforementioned mechanical parameters are showcased. It is worth noting that the elastic constants were computed from the linear section of the axial

stress-axial strain curve. Finally, the complete stress-strain curves of the ten rock samples are thouroughly presented in the Appendix.

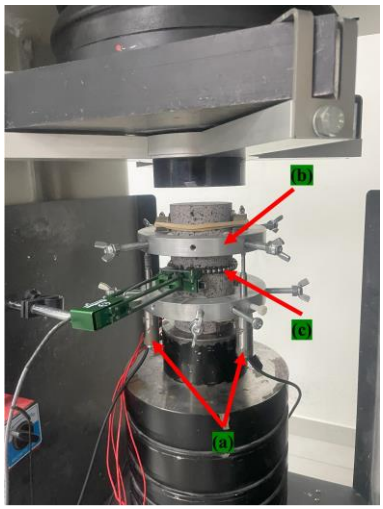

Figure 4. The laboratory loading apparatus: (a) the LVDTs; (b) the aluminium ring; (c) the circumferential chain extensometer.

Table 2. The mechanical properties of the ten rock samples.

Rock type	Specimen name	Compressive strength (MPa)	Young's modulus (GPa)	Poisson's ratio
Marble	M1	118.23	41.27	0.30
	M2	110.62	40.78	0.40
	M3	122.42	44.35	0.33
	M4	84.54	42.85	0.32
	M5	142.59	50.84	0.32
	M6	104.26	41.66	0.35
	M7	92.65	50.00	0.22
	M8	113.52	46.51	0.45
Basalt	B1	58.77	12.19	0.16
	B2	80.65	19.96	0.15

4. Existing Techniques for Predicting the Crack Initiation Threshold

In this section of the paper a brief review will be provided on the methods that have been suggested over the years for identifying the CI stress threshold for rock-type material. The methods will be presented in the following order, starting with the volumetric strain-based approaches, moving next to the lateral strain-based techniques, then to the axial strain-based technique, and finally to the instantaneous Poisson ratio method, as well as geophysical monitoring techniques, like Acoustic Emissions (AE). The aim of this section is to merely mention the empirical techniques, most of which will be utilized in the preceeding paragraphs of the study, and to state the main critism that each one of them has faced. For a more in-depth critical review of the existing methods capable of predicting the CC, CI, and CD stress thresholds the author suggests reading the work of Zhang et al. [24].

4.1. Volumetric Strain Methods

The earliest attempt for determining the onset of stable crack growth of a rock specimen during a compressive test was proposed by Brace et al. [1] almost 60 years ago. Particulalry, by observing the stress-strain cuvres of three different rock specimens, specifically a granite, a marble, and an aplite, they came to the conclusion that the CI stress threshold coincides with the point of deviation from linearity of the axial stress-volumetric strain curve. The method is showcased in Figure 5a. The obvious issue of the empirical technique are the imminent subjective errors that arise when the CI stress is determined, since the user must determine the point of departure from linearity of a curve via the naked eye.

Close to three decades later, Martin and Chandler [5] proposed the Crack Volumetric Strain (CVS) method, which involved plotting the crack volumetric strain as a function of the axial strain as it can be seen in Figure 5b. The moment where dilatancy commences is assumed to correspond to the CI stress. Moreover, the crack volumetric strain is computed from the following formula:

$$\varepsilon_V^{cr} = \varepsilon_V - \frac{1-2v}{E}\sigma_1 \tag{2}$$

where, ε_V^{cr}: represents the crack volumetric strain, v: denotes Poisson's ratio, E: symbolizes Young's modulus, and σ_1: is the maximum principal stress. Although the method is less subjective than it's predeccesor, it has been heavily criticised by the fact that the predicted CI stress is influenced by the values of the two elastic constants [6].

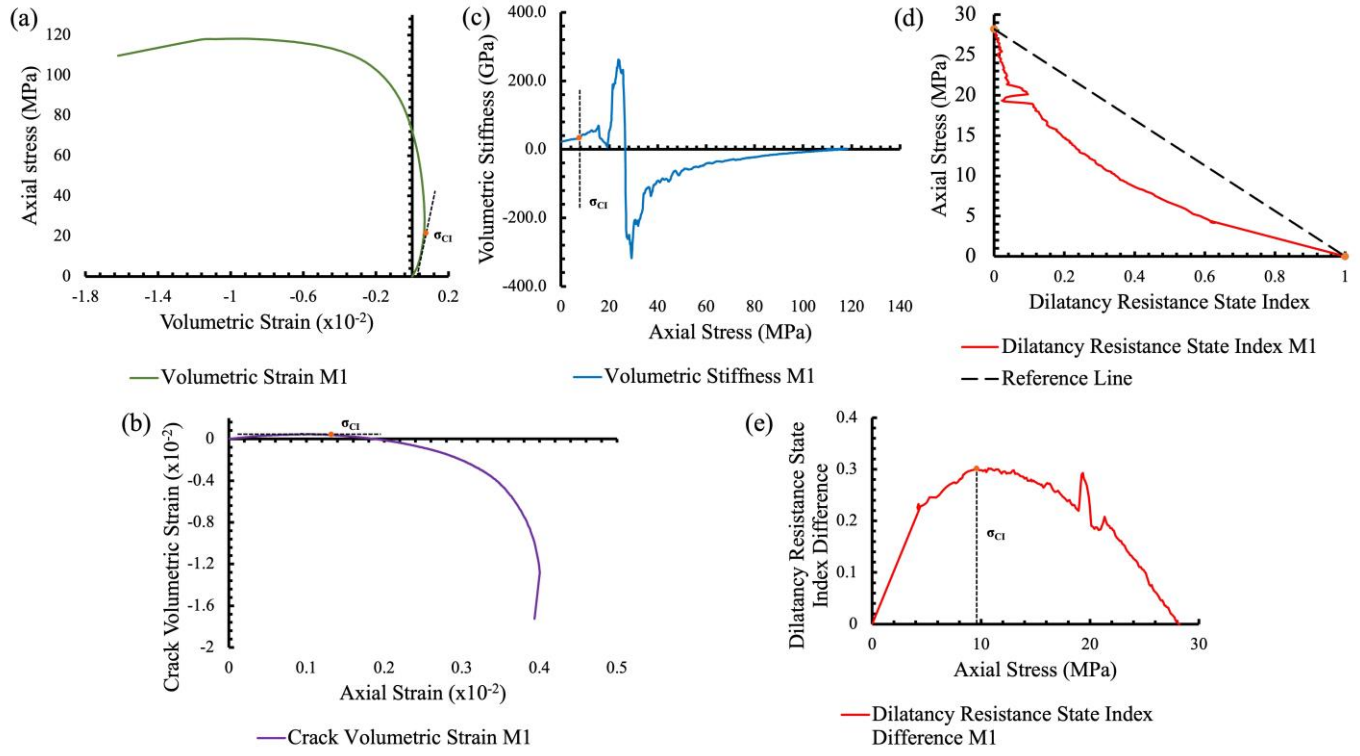

Figure 5. (a) The method of Brace et al. [1]; (b) the CVS technique; (c) the moving point regression method; (d) and (e) the VSR method.

A few years later, Eberhardt et al. [6] proposed a moving point regression technique (as well as AE monitoring, which will be discussed in section 4.5) in order to detect the stable crack growth threshold of Lac du Bonnet granite. Particulalry, the researchers suggested plotting the volumetric stiffness versus the axial stress, and supported that the CI stress threshold is the point of the curve which corresponds to the end of a linear elastic region before some minor irregularities commence in the form of the curve. The application of the method can be seen in Figure 5c. Overall, the moving point regression technique insert a very high degree of subjectivity. More recently, Li et al. [14] suggested the Volumetric Strain Response (VSR) method, which firstly requires to compute the dilatancy resistance state index from the following expression:

$$\delta_{CI} = 1 - \frac{\varepsilon_V}{\varepsilon_V^{CD}} \quad (3)$$

where, δ_{CI}: is the dilatancy resistance state index, and ε_V^{CD}: denotes the volumetric strain that corresponds to the CD. The latter threshold can be easily defined by the maximum point of the axial stress-volumteric strain curve. Moreover, once the dilatancy resistance state index has been calculated the authors suggest plotting the axial stress as a function of the index. Then a reference line must be drawn that connects the maximum dilatancy resistance state index value with the CD stress point. Finally, the difference in dilatancy resistance state index values between the reference line and the curve must be computed and lastly plotted as a function of the axial stress. The stress point that corresponds to the maximum difference is considered to be the CI threhold. Figures 5d and 5e showcase the application of the VSR method. The technique is fairly new and as a result it hasn't been applied to many rock types in order for it's weaknesses to become apparent yet. However, it is worth mentioning that some researchers support that the volumetric strain curve is inappropriate for the accurate determination of the CI stress, in comparison with the lateral strain curve, because generally the lateral strain is more sensitive to the propagation of cracks, prior to the CD threshold [8].

4.2. Lateral Strain Methods

The first attempt at utilizing the lateral strain curve for the predicting of the CI stress dates back to the work of Lajtai [3]. The latter author suggested that the onset of stable crack growth corresponds to the point of deviation from linearity of the axial stress-lateral strain curve. The application of the method can be seen in Figure 6a below. Similalry to some of the previous empirical techniques, this one also suffers from subjective errors, because the user must determine the point of departure from linearity from a curve that can be highly non-linear in its entirety [8,20].

A few years later, Stacey [4] proposed his well known extentiosal strain criterion, in an attempt to acurately analyze the sudden rock failures that were observed in some deep South African gold mines. The criterion essentially involved plotting the lateral strain as a function of the axial strain. The CI threshold is assumed to coincide once again with the point of deviation from linearity of the aforesaid curve. The technique is showcased in Figure 6b. Likewise with the previous method, the CI stress cannot be predicted accurately and consistently due to the high degree of subjectivity.

Three decades later, Nicksiar and Martin [8] published their celebrated paper where they proposed the well renowned Lateral Strain Response (LSR) method. This simple approach firstly involved connecting a reference line from the point of zero stress to the point of unstable crack growth (i.e. the CD stress) in the axial stress-lateral strain curve. They next recommended computing the differences between the lateral strains of the curve and the reference line, and finally plotting them versus the axial stress. The authors supported that the maximum calculated difference is considered as the CI stress. The two necessary charts for the application of the technique can be seen in Figures 6c and 6d. The method is completely objective, however it has been observed that it yields accurate results only when the stiffness of the elastic part of the lateral strain curve is greater than the slope of the reference line [12]. When this condition is not met the predicted CI stress value is imprecise.

Wen et al. [11] presented the Relative Compression Strain Response (RCSR) method that depended on the calculation of the relative compression strain, the latter is given by the following expression:

$$\varepsilon_l^C = 1 - \frac{\varepsilon_l}{\varepsilon_l^{CD}} \quad (4)$$

where, ε_l^C: denotes the relative compression strain, and ε_l^{CD}: signfies the lateral strain value that corresponds to the CD. Once the relative compression strain is computed it must be plotted as a function of the axial stress. After that a reference line must be drawn from the CD stress to the maximum relative compression strain value, i.e. 1. Finally, the authors propose to calculate the difference in relative compression strain values between the reference line and the curve, and subsequently plot them versus the axial stress. Similalry, to the LSR method the maximum difference is regarded as the CI stress. The application of the technique can be seen in Figures 6e and 6f. Like it's predecessor the technique eliminated subjective errors, but it has been proven that it yields the results of the LSR method divided only by a constant, particulalry the oposite value (i.e. the positive value) of the lateral strain that corresponds to the CD [12]. Consequently, the two methods are essentailly the same [12].

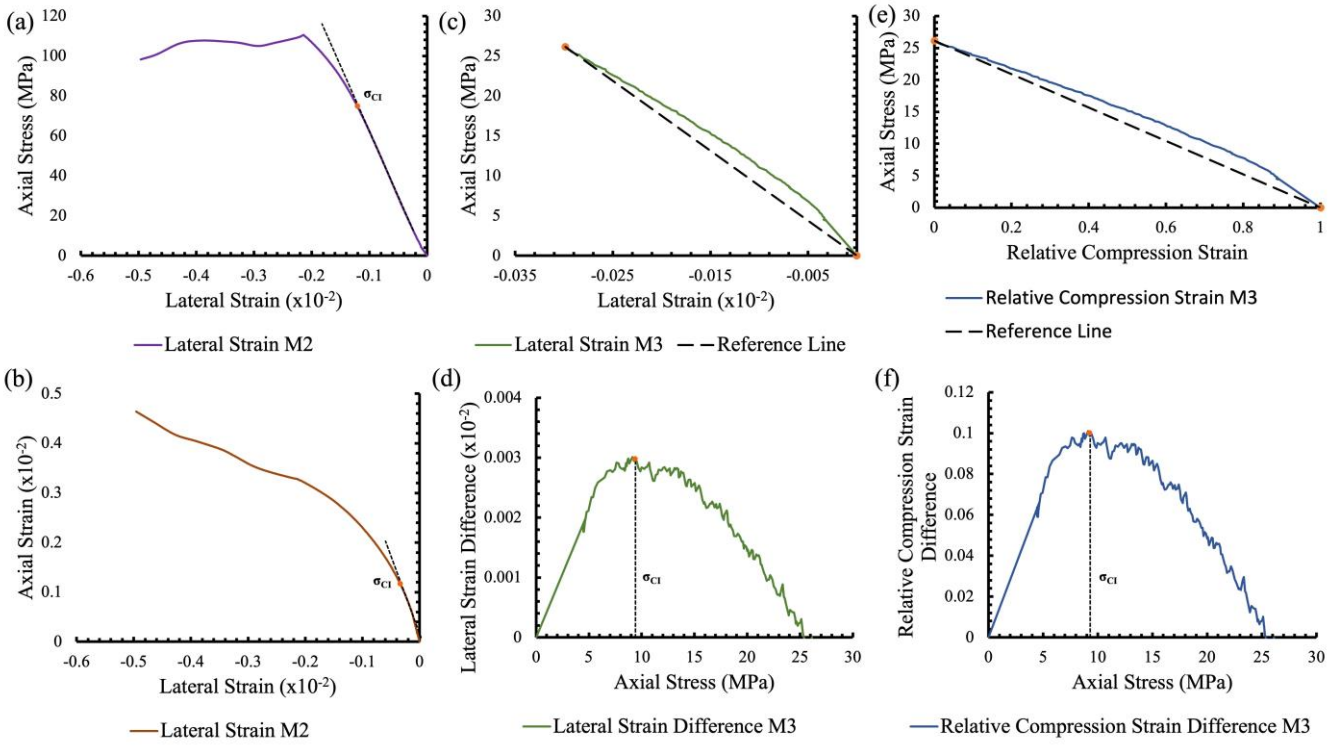

Figure 6. (a) The method of Lajtai [3]; (b) the technique of Stacey [4]; (c) and (d) the LSR method; (e) and (f) the RCSR method.

Finally, Tang et al. [12] published an improved version of the LSR method which is called the Lateral Strain Interval Response (LSIR) method that essentially combatted the aforesaid weakness of the LSR technique by altering the two endpoints of the reference line. Specifically, the researchers supported that the upper bound of the reference line should be as close to the CI stress as possible, while the lower should match with the CC stress. Once again, the difference in lateral strain values between the reference line and the lateral strain curve must be computed and plotted as a function of the axial stress. The maximum difference is considered to correspond to the onset of stable crack growth. In Figures 6g and 6h the implementation of the method is displayed. The main drawback of the technique, according to the authors opinion, is the fact that the user must have a somewhat rough estimate of the CI threshold prior to the utilization of the method, in order to properly set the upper bound of the reference line. Hence, the LSIR method can serve as a possible improvement of the estimation of the CI stress, if especially high accuracy is needed.

4.3. Axial Strain and Instantaneous Poisson's Ratio Methods

Recently, Wen et al. [13] suggested a new empirical technique that is called the Axial Crack Strain (ACS) expansion rate method. The method firstly involves computing the axial crack strain from the following formula:

$$\varepsilon_a^{cr} = \varepsilon_a - \frac{1}{E}\sigma_1 \tag{5}$$

where, ε_a^{cr}: denotes the axial crack strain. Furthermore, the next step requires to compute the axial crack expansion rate from the equation below:

$$u_a^{cr} = \frac{d\varepsilon_a^{cr}}{dt} \tag{6}$$

where, u_a^{cr}: symbolizes the axial crack expansion rate, and t: is the loading time. Once the latter is calculated it must be plotted as a function of axial stress. The point where the axial crack expansion rate becomes negative is considered as the CI stress. Alternatively, the axial crack strain can be plotted versus the axial stress, and subsequently the onset of stable crack crack growth coincides with the point where dilatation commences (this approach yielded more realistic results). The application of the method is showcased in Figures 7a. Although the empirical technique overcomes the issue of subjectivity, the CI stress threshold is heavily influenced by Young's modulus.

Diederichs [7] suggested the instantaneous Poisson's ratio method that essentially involved plotting the latter as a function of the axial stress in logarithmic scale. The CI stress is considered as the point of deviation from linearity of the curve. In Figure 7b below the implementation of the technique is showcased. Although the method deviates from the classical strain-based approaches it does not eliminate subjective errors.

4.4. Acoustic Emission Methods

As it was mentioned earlier, Eberhardt et al. [6] in his celebrated paper also utilized Acoustic Emission (AE) signals to determine the CI stress, mainly based on the concept that prior to the onset of stable crack growth very few AE signal hits are produced within the rock sample. Consequently, the researchers suggested plotting the AE hits as a function of the axial stress, with the stress point correspoding to the first recorded hits being considered as the CI stress. The application of the method is shown in Figure 8a. The main drawback of AE monitoring as a whole is that the received signals may be heavily disturbed, if not produced entirely, by background noises [8]. Moreover, it has also been observed that some hard rocks produce little to none AE activity prior to reaching their peak strength [13].

Almost one decade later, Zhao et al. [9] proposed to plot the cumulative AE hits, that were recorded during the compressive test, as a function of the axial stress. The authors supported that the point of departure from linearity of the curve corresponds to the onset of stable crack growth. The methodology is presented in Figure 8b below. Apart from the above-mentioned weaknesses of all the AE monitoring techniques, this one also has imminent subjective inaccuracies.

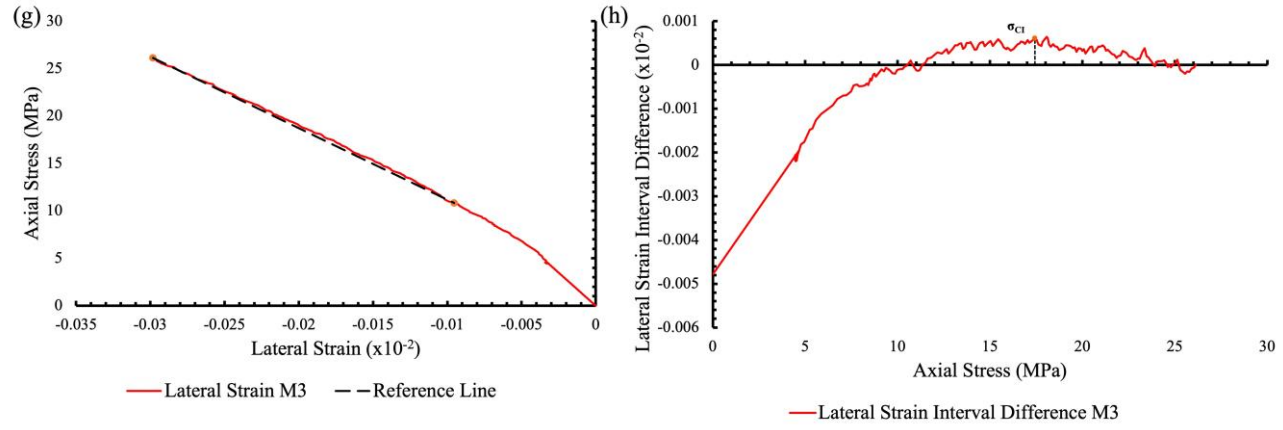

Figure 6. (continued) (g) and (h) the LSIR method.

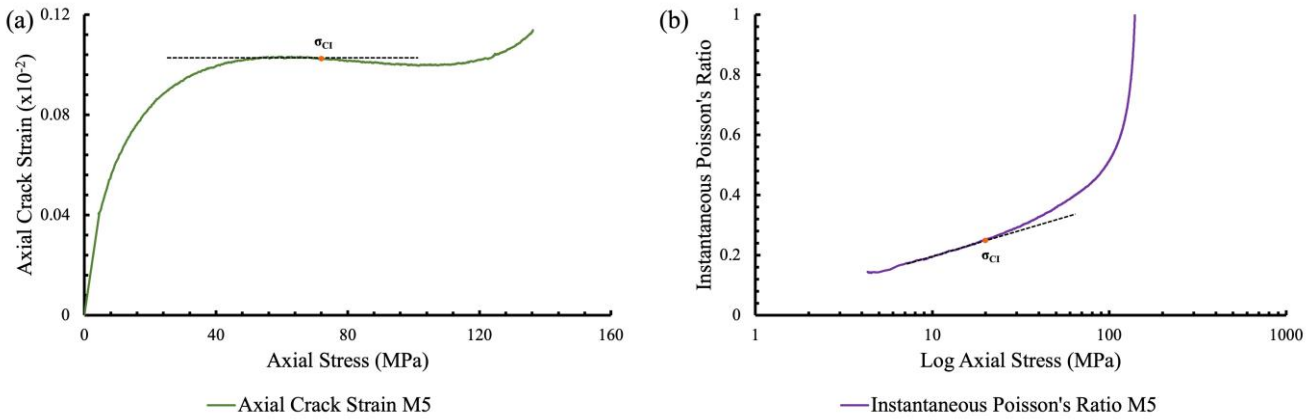

Figure 7. (a) The ACS method; (b) the instantaneous Poisson's ratio method.

Finally, a few years later Zhao et al. [10] made an attempt to improve the previous method by eliminating its subjectivity. The authors began by assuming that the cumulative AE hits-axial stress curve displays a characteristic S-shape form. Moreover, the first step of the method requires picking a random point on the initially increasing part of the cumulative AE hits-axial stress curve, and then drawing several references lines from the zero stress point to the UCS. Subsequently, the upper end point of the reference line with the smallest slope is regarded as the upper boundary. The next step involves once again drawing several reference lines from the upper boundary till the initial random point. Similalry, the lower endpoint of the reference line with the smallest slope is defined as the lower boundary. The authors then suggest computing the difference in cumulative AE hits values between the reference line and the curve, and plotting the results versus the axial stress. The maximum difference corresponds to the CI stress. The application of the technique can be seen in Figures 8c, 8d, and 8e. In addition to the fact that the method is a bit complicated, the author has also noticed that the initial assumption that the curve has an S-shaped form, is not always met.

5. Trapezoid Rule Method

Through the short, but necessary, litterature review of the previous section it is easily comprehended that any new methods that are suggested for the determination of the CI threshold must fill some specific criteria, in order to advance the research field. Particulalry, new techniques must totally exclude subjective errors, possess a robust and clear physical explanation, while also combine easy implementation from the user.

Having these points in mind the author developped two new method, one being presented in this part of the study while the second in part II, that are both based in elementary mathematical theorems. The first method, which will be presented in this part of the study, is specifically based on the Trapezoid Rule (or Trapezium Rule) (TR). The latter is essentially an elementary approach that can approximate the area under a curve, instead of using the classical definite intergration method. Consequently, overall the method relies on the computation of the area under the axial stress-lateral strain curve through the TR approximation for the determination of the CI stress. The usage of the axial stress-lateral strain curve, rather than the other two curves that are available, is due to the general acceptance that the lateral strain is far more sensitive to the propagation of cracks, prior to the onset of unstable crack growth [8].

The steps of the TR method can be broken down as follows. Firstly, the area under the curve, up until the CD stress, must be divided into small trapezium strips, as it can be seen in Figure 9a. Generally, the CD stress can be accurrately determined by the maximum point of the volumetric strain curve. Moreover, it is worth noting that strips should be divided depending on the number of data that were acquired from the compressive test. Namely, if n_k lateral strain points were collected prior to the onset of unstable crack growth, the area should be divided in $n_k - 1$ trapezium strips (i.e. the maximum strips possible), the higher the number of strips the more accurate the approximation. In the next step, the area of each trapezium strip should be computed, by applying the TR approximation as it is written by the following expression:

$$\int_{\varepsilon_l^a}^{\varepsilon_l^b} \sigma(\varepsilon_l) d\varepsilon_l \approx \frac{1}{2}(\varepsilon_l^b - \varepsilon_l^a)\{\sigma(\varepsilon_l^a) + \sigma(\varepsilon_l^b)\} \quad (7)$$

where, ε_l^b, ε_l^a: denote the final and the first lateral strain values of two endpoints of a trapezium strip, respectively, $\sigma(\varepsilon_l)$: is the axial stress-lateral strain curve equation for the trapezium strip under consideration, and $\sigma(\varepsilon_l^a)$, $\sigma(\varepsilon_l^b)$: symbolize the axial stress values that correspond to the lateral strain values ε_l^a and ε_l^b, respectively. Subsequently, the area of the first strip should be added with the area of the next and the sum of the two first strips with the area of the third, and so forth, up until the hole area under the curve (up until the CD stress) is computed. In this way, by plotting the constant summation of the strips until the onset of unstable crack growth as a function of the axial stress, a pathway is essentially created which showcases the increasing nature of the area under the curve.

Due to the form of the axial stress-lateral strain curve, the aforesaid increase should initially be linear and very quick. However, the curve after a point deviates from linearity and subsequently enters an non-linear region that can be characterised as concave, as a result, the rate of increase of the area should behave similalry. Ultimately, once the plotted curve of the gradual summation of the area under the curve deviates from linearity it can be considered as the CI stress threshold. This point can be determined objectively by connecting a reference line between the zero point of the graph and the total area under the lateral strain curve up until the CD, and calculating the differences between the values of the reference line and the curve. The maximum difference coincides with the CI stress. The application of the method can be seen graphically in Figures 9b and 9c.

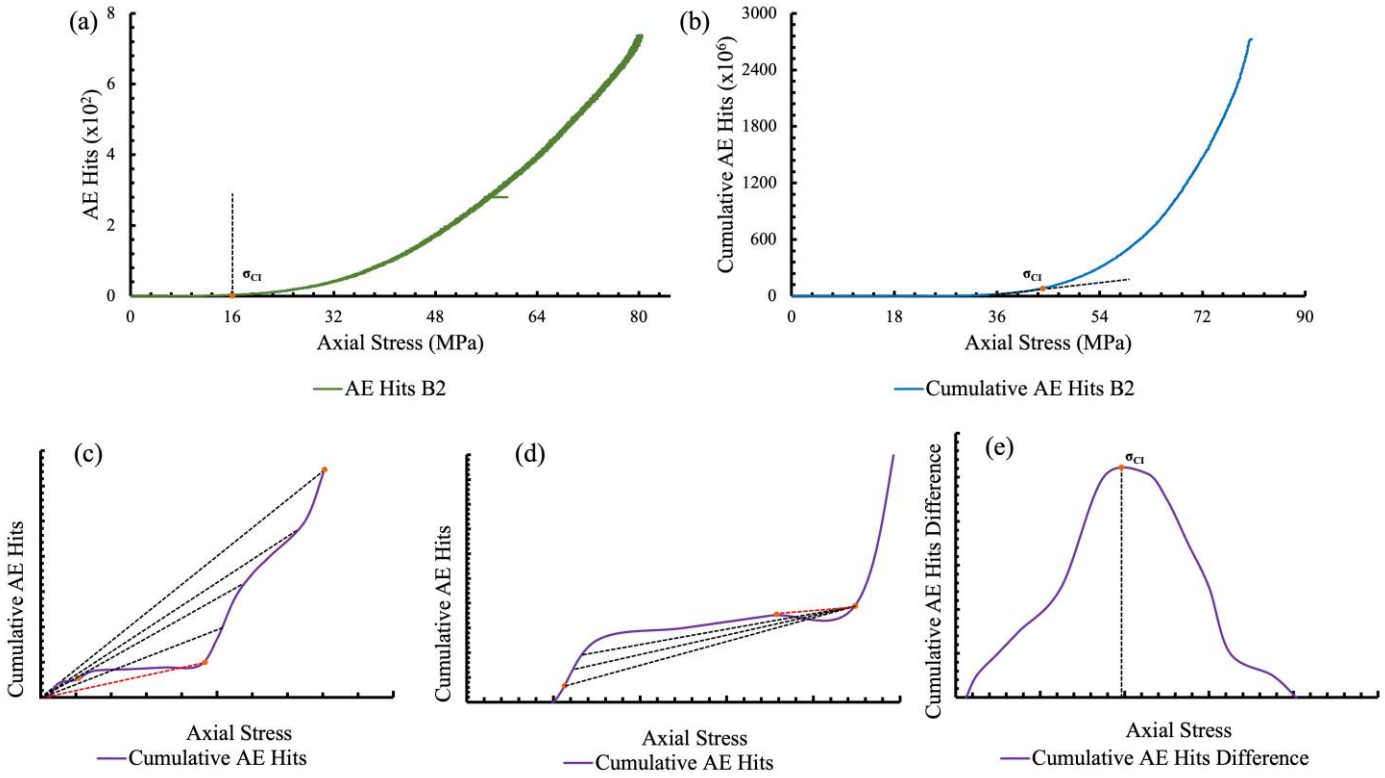

Figure 8. (a) The method of Eberhardt et al. [6]; (b) the technique of Zhao et al. [9]; (c)-(e) cartoonish representation of the method of Zhao et al. [10].

However, a physical rationale that bridges the gap between the microcrack initiation of the rock and the integrated lateral strain energy is yet to be provided. As it is well understood, through the TR approximation the area under the lateral strain curve is computed, i.e. the lateral strain energy. The latter is then plotted as a function of the axial stress and the point from deviation from linearity of the previous curve is considered as the CI stress. According to the influential energy-based fracture mechanics theory of Griffith [25,26], in order for a crack to propagate there must be an increase in surface energy, so that a new crack surface may form. This necessary increase is subsequently supplied by a decrease in strain energy. Through this thermodynamical approach the physical explanation of the TR can be given. Particularly, as it can been seen from Figure 9b the lateral strain energy initially increases linearly with the applied axial stress and this energy is stored in its entirety as strain energy within the rock sample. As cracks commence to spread (i.e. the CI threshold is reached) a portion of the created lateral strain energy, due to the loading, must be provided to the surface energy, in order for the new crack surfaces to form. Consequently, the response of the curve ceases to be linear and a concave segment commences, essentially showcasing a general increase in strain energy but with a decreasing rate, since not all the created strain energy is stored because a part of it is given to the surface energy. Ultimately, through this classical energy-based theory of brittle fracture it can be easily accepted that the departure from linearity of the lateral strain curve can be considered as the CI stress.

Overall, the proposed energy-based method can more accurately represent the onset of crack propagation, in comparison to the more classical strain-based approaches, because it directly takes into account the well-renowned fracture mechanics theory of solids of Griffith [25,26]. In contrast, the strain-based techniques that were discussed in the previous section mostly relied on empirical observations from laboratory testing, and subsequently lacked a robust and clear micromechanical explanation.

Collectively, now that the physical explanation of the TR method has been given, the basic steps for its implentation can be summerized as follows. Divide the area under the axial stress-lateral strain curve, until the CD stress, into small trapezium strips (the maximum strips possible). Compute the area under each strip by utilizing the TR approximation, hence the right hand side of Equation (7). Gradually sum the areas under each strip, one by one, and plot them as a function of the axial stress. Connect a reference line from zero point of the chart till the total area under the curve, up until the CD stress, and compute the difference of the area values between the curve and the reference line. Plot the difference versus the axial stress, the maximum difference is regarded as the onset of stable crack growth, i.e. the CI stress.

6. Application and Validation of the Trapezoid Rule Method

In this section of the paper the TR method will be utilized to predict the CI stress threshold of the ten tested rock specimens, and subsequently the yielded results will be compared with those produced by the already established empirical techniques, that were shorlty presented above. In this way, it will be made clear whether the TR method is a viable technique that can accurately predict the onset of stable crack growth of rock-type material.

It is worth noting however that all methods that were prone to subjective errors (e.g. [1,3-4,6-7,9]) where completely excluded from the aforesaid process, due to their anticipated inaccuracy. Additionally, the ACS method could not be applied, because the results that were produced were paradoxical since they indicated that the CI stress was greater than the CD stress. Moreover, specifically for the two basaltic samples the CVS method was incapable of determining the CI stress, propably due to the high number of pre-existing cracks (in this case voids) that were present within the specimens [6,8]. Particulalry, it was observed that dilatation, i.e. the onset of stable crack growth, commenced from the beginning of the compressive test. Furthermore, the RCSR technique was also totally excluded because it yielded the exact same results as the LSR method, consequently it was choosen to include only the LSR method because it was published earlier than the RCSR technique. Finally, AE monitoring techniques were not applied, since the received signals can be heavily distrubed by background noises hence greatly influencing the predicted CI stress.

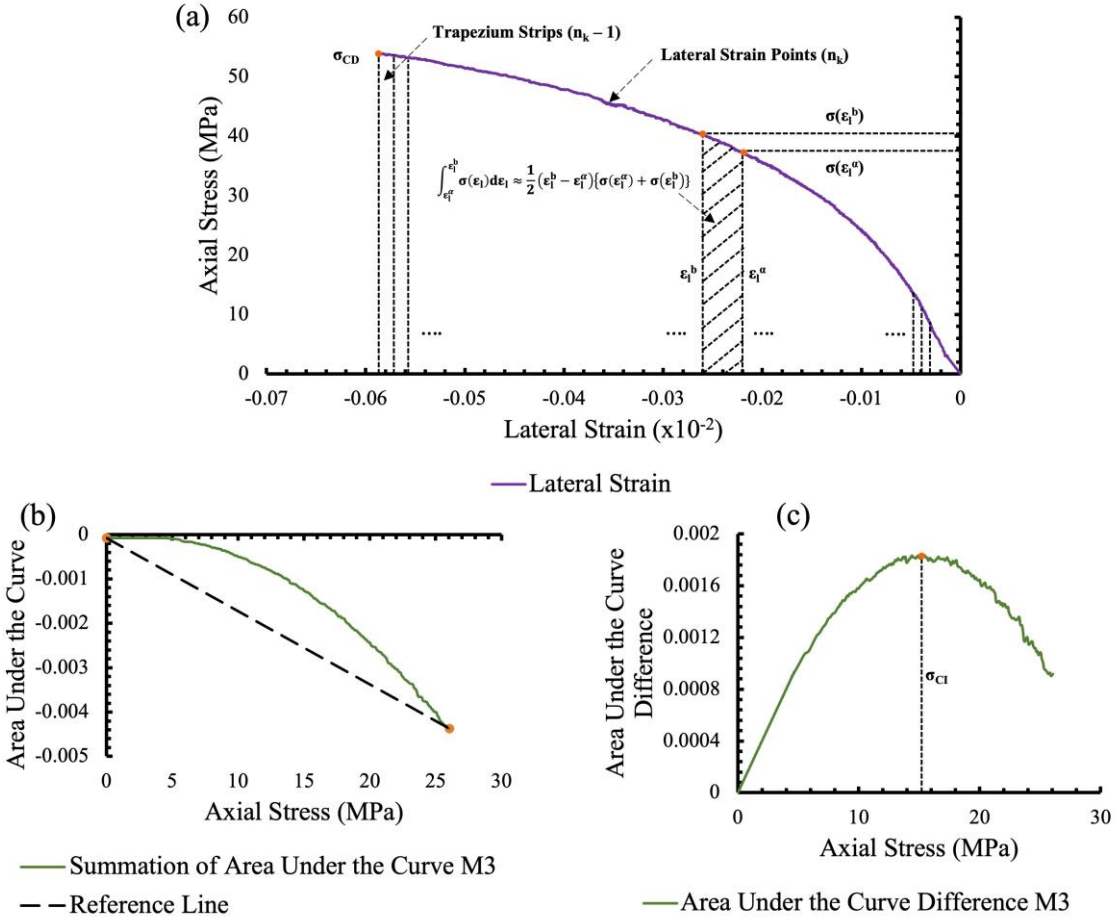

Figure 9. (a) The general cartoonish representation of the TR method; (b) the gradual summation of the area of the trapezium strips; (c) the calculated difference in area values between the reference and the curve from (b).

In the following table below the determined CI stress values, as well as the CD stress, for the ten rock specimens are showcased. In addition, the difference in CI to UCS ratio value between the newly suggested TR method and the other techniques was computed, and is subsequently presented in Table 3. Specifically, the mean difference between the LSR and the TR method for the marble and basaltic specimens was approximately 3.20 % and 1.56 %, respectively. Indicating that the CI stress values predicted by the two methods where especially close. Moreover, the mean computed difference between the LSIR and the TR method for the marble samples was around 4.22 %, thus both methods demonstanted similar results. However, the mean difference for the same two techniques for the two basaltic rocks was relatively high, and specifically close to 24.45 %. Furthermore, once again the mean difference between the VSR and the new method for the marble samples was around 4.27 %, hence the two techniques display a high correlation. While the mean difference for the basaltic rocks was estimated at a modest 16.22 %. Finally, the mean difference between the CVS and the TR method was approximately 3.09 %, therefore the two methods had exceptionally close results. It is also noteworthy that for statistical reasons the Standard Deviation (SD), for each rock type, is showcased in Table 3.

7. Discussion

According to the findings of the previous section, it was made clear that the newly suggested TR method showcased exceptionally close results with all four frequently used empirical techniques, i.e. the LSR, LSIR, VSR, and the CVS methods, for the eight marble samples. Consequently meaning that the TR technique can successfully and accurately predict the CI stress for the latter rock type. Additionally, the TR method had very similar results with the LSR method for the two basaltic rocks. However, the proposed mathematical technique displayed dissimilar results with the LSIR and the VSR methods for the two basaltic specimens, thus raising concerns whether the method is appropriate for the current rock type.

Firstly, the bad correlation of the TR and the VSR method for the vesicular basalts is most likely attributed to the unique shape of the volumetric strain curve, which prompts the author to support that the utilization of the VSR technique for the determination of the CI stress is inappropriate. The axial stress-volumetric strain curves of the two basaltic specimens are shown in Figures 10a and 10b. Particulalry, as it can be easily observed prior to the onset of unstable crack growth, i.e. the reversal point of the curve, the curves display two distinct linear regions. Once the first such region deviates from linearity the onset of stable crack growth begins, according to Brace et al. [1]. Essentially, the ultimate aim of the VSR method is to predict the aforesaid point objectively by using the reference line, in order to compute the difference between the values of the reference line and the curve. However, in the case of the two basaltic rocks the maximum difference does not coincide with the departure from linearity of the first elastic region, but rather the second. As a result, the large differences between the TR and the VSR method are justfied, since the latter does not essentially predict the CI stress threshold, due to the unique shape of the volumetric strain curve of the vesicular basalts.

As for the significantly increased differences that were apparent between the TR and the LSIR method for the two basalts, these can be explained by the relation of the stiffness of the elastic part of the lateral strain curve and the slope of the reference line. Particulalry, the latter was greater than the last. As a result, the application of the LSIR technique was unnecessary in the first place, since the LSIR was proposed with the aim to improve the LSR method when the aforementioned relation between the slopes of the curve and the reference line was not met. The lateral strain curves, along with their respective reference lines for the two vesicular basalts are given in Figures 10c and 10d. Therefore, as long as the LSR method can predict the CI stress accurately, and since it exhibits very close results with the TR technique, it can be safely assumed that the last method can be applied with high precision to the basaltic specimens, despite its bad correlation with the LSIR technique, which was redundant to utilize anyways.

Moreover, it is also worth noting that both the VSR and the LSIR methods were applied and validated using limestones and granodiorites, respectively. Neither technique utilized vesicular basalts, thus possibly meaning that the two previous methods may be inappropriate for the latter rock type. Additionally, it can be easily observed that in general the CI stress threshold that was determined by the methods for the two basalts displayed a very high dispersion. Particularly, the mean CI stress across all the methods for basalts B1 and B2 was around 34.18 MPa and 44.68 MPa, respectively. The SD was excessively high for the two specimens, specifically 9.37 MPa for B1 and 13.53 MPa for B2. Consequently, more vesicular basalts need to be tested in the future so that a clear conclusion can be drawn as to which method can more accurately determine the CI threshold for that rock type.

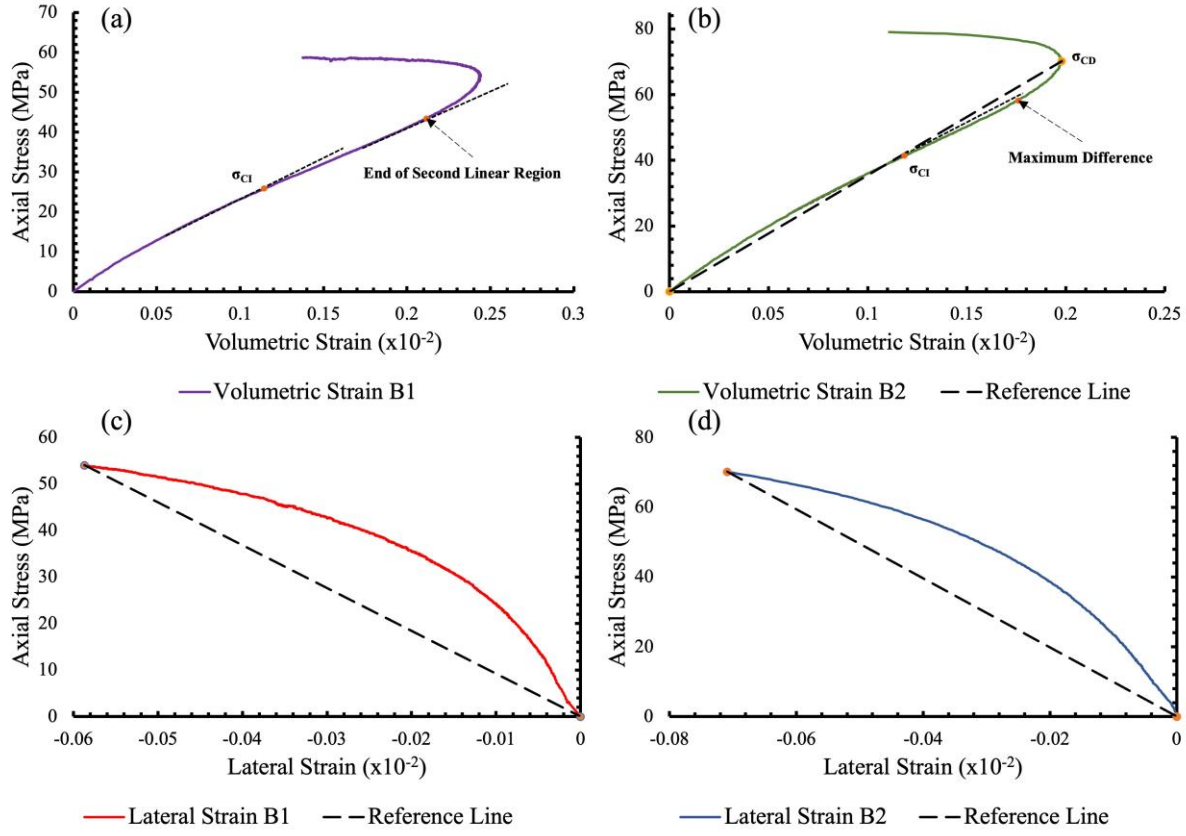

Figure 10. (a) and (b) The volumetric strain curves of the two basaltic rocks; (c) and (d) the lateral strain curves of the basalts.

Table 3. The predicted CI stress threshold using different methods.

Rock Specimen Designation	CD (MPa)	TR	LSR		LSIR		VSR		CVS	
		CI (MPa)	CI (MPa)	Difference (%)	CI (MPa)	Difference (%)	CI (MPa)	Difference (%)	CI (MPa)	Difference (%)
M1	28.20	19.23	19.34	0.09	19.34	0.09	9.54	8.20	19.34	0.09
M2	29.33	12.96	8.57	3.97	23.75	9.75	9.38	3.24	19.58	5.98
M3	26.13	15.44	9.12	5.16	18.06	2.14	9.04	5.23	18.06	2.14
M4	24.69	12.20	5.70	7.69	5.70	7.69	7.36	5.73	15.82	4.28
M5	31.35	13.60	12.46	0.80	19.54	4.17	9.42	2.93	17.42	2.68
M6	18.73	11.89	9.43	2.36	8.11	3.63	8.13	3.61	12.53	0.61
M7	23.94	12.28	9.32	3.63	17.34	5.03	8.32	4.71	15.43	2.97
M8	15.90	6.60	8.05	1.28	8.05	1.28	5.99	0.54	13.36	5.95
B1	54.08	35.09	34.42	1.14	22.17	21.98	45.05	16.95	-	-
B2	70.18	47.03	45.43	1.98	26.72	25.18	59.52	15.49	-	-
Mean Marbles	24.78	13.08	10.25	3.12	14.99	4.22	8.40	4.27	16.44	3.09
Mean Basalts	62.13	41.06	39.93	1.56	24.45	23.58	52.29	16.22	-	-
SD Marbles	5.26	3.55	4.12	2.52	6.69	3.24	1.24	2.26	2.62	2.21
SD Basalts	11.38	8.44	7.79	0.60	3.22	2.26	10.23	1.03	-	-

Furthermore, in future studies it would be of particular interest to investigate the influence of various rock heterogeneity parameters, such as grain size and mineralogy, on the results produced by the suggested TR method. Additionally, the newly proposed TR method should be applied to more rock types of varying porosity (i.e. granites, karstified limestones, andesites, diorites), in order to assess whether the technique can be accurately utilized across all rock types.

Similarly with the suggestion of Tang et al. [12] for the improvement of the LSR method, the usage of different endpoints for the reference line were tested, in order to investigate whether the results of the TR method could more closely match those of the other frequently used methods. Thus essentially applying a Trapezoid Rule Interval (TRI) method. Likewise with the LSIR method, the lower bound was set as close as possible to the CC stress, while the upper bound was kept at the CD stress threshold. For the ten specimens of the present study alterations in the upper and lower bounds of the reference line did not produce closer differences, but rather larger ones. However, this may be material dependent, consequently in other frequently encountered rock types, such as limestones, granites, andesites etc., selecting different endpoints for the reference line may greatly improve the results of the TR method.

8. Conclusions

In part I of this study, the generally accepted fracturing process of brittle rocks that are subjected to compressive tests was thoroughly outlined. Additionally, the practical importance of the CI stress was highlighted, since it is considered as a more realistic threshold for the in-situ spalling strength of the rock mass. The determination of the onset of stable crack growth has troubled researchers for many years. Consequently, many empirical methods have been proposed over the past six decades for its accurate prediction. The majority of the techniques utilize the stress-strain curves that are obtained from a compressive test, while some others apply geophysical monitoring methods, i.e. AE monitoring. The aforesaid methods were briefly presented, and their respective weaknesses were stated.

Subsequently, the main aim of this paper was to introduce a new method based on an elementary mathematical calculus approximation known as the Trapezoid Rule. The latter newly suggested technique involved dividing the area under the axial stress-lateral strain curve, up until the CD stress, into small trapezium strips and computing their areas using the TR approximation. The next step required to gradually sum the area of each strip and plot them as a function of the axial stress. In this way, the increasing pathway of the area under the lateral strain curve is more easily visible. Once this increase of the area deviates from linearity, i.e. the lateral strain curve departs from linearity, the CI stress is reached. The aforementioned threshold was determined by drawing a reference line from the zero point of the chart till the CD stress, and subsequently computing the difference between the curve and the reference line. The maximum difference corresponds to the onset of stable crack growth.

The TR method was applied and compared with the frequently utilized empirical methods of the existing literature, using eight marbles and two vesicular basalts. Ultimately, the TR method yielded exceptionally close results with the LSR, LSIR, VSR, and CVS for the eight marble specimens, with the overall computed differences of the TR and the four other methods being less than 4.3 %. Thus showcasing that the TR technique can accurately determine the onset of stable crack growth of marbles. Similarly, the TR method displayed very close results with the LSR technique for the two basalts. On the contrary, it had a poor correlation with the VSR and the LSIR methods for the same rocks. The unsimilar predicted thresholds with the latter were mainly attributed to the unique shape of the volumetric strain curves of the basalts, that essentially rendered the VSR method as ineffective. While the augmented differences with the last were credited to the relation between the stiffness of the elastic part of the lateral strain curve and the slope of the reference line. Particularly, according to the own words of Tang et al. [12]: ''… *When the stiffeness of the elastic stage is greater than the slope of the reference line, the LSR method can accurately determine the crack initiation stress.* …''. Consequently, the aim of the LSIR method was to improve the results of the LSR method when the previous condition was not met. However, in the case of the two basalts the condition was satisfied, hence the usage of the LSIR method was redundant in the first place. Therefore, since the TR and the LSR methods had especially close results, the latter can also accurately determine the CI stress of two basaltic rocks.

Future research should most definitely test the accuracy of the TR method in other usually encountered rock types, such as granites, diorites, limestones, and sandstones. Furthermore, more vesicular basalts should also be tested, in order to safely acknowledge that the TR technique can correctly predict the CI stress for that rock type.

In part II of this study, one more method for the determination of the CI stress will be introduced, applied and subsequently validated, using the same rock specimens as part I. The method of part II is once again based on an elementary mathematical theory of calculus, and particulalry the second derivative.

Acknowledgments

No funding was received to assist with the preparation of this manuscript. The author would like to acknowledge S. Markopoulou and M.A. Marouli for their help in language editing of this paper.

Conflicts of Interest

All the authors claim that the manuscript is completely original. The authors also declare no conflict of interest.

Data availability

All relevant data related to this manuscript are available and can be provided upon reasonable request.

Appendix A1

In Figure 11 below the complete stress-strain curves which were obtained from the compressive tests of the ten rock specimens are presented.

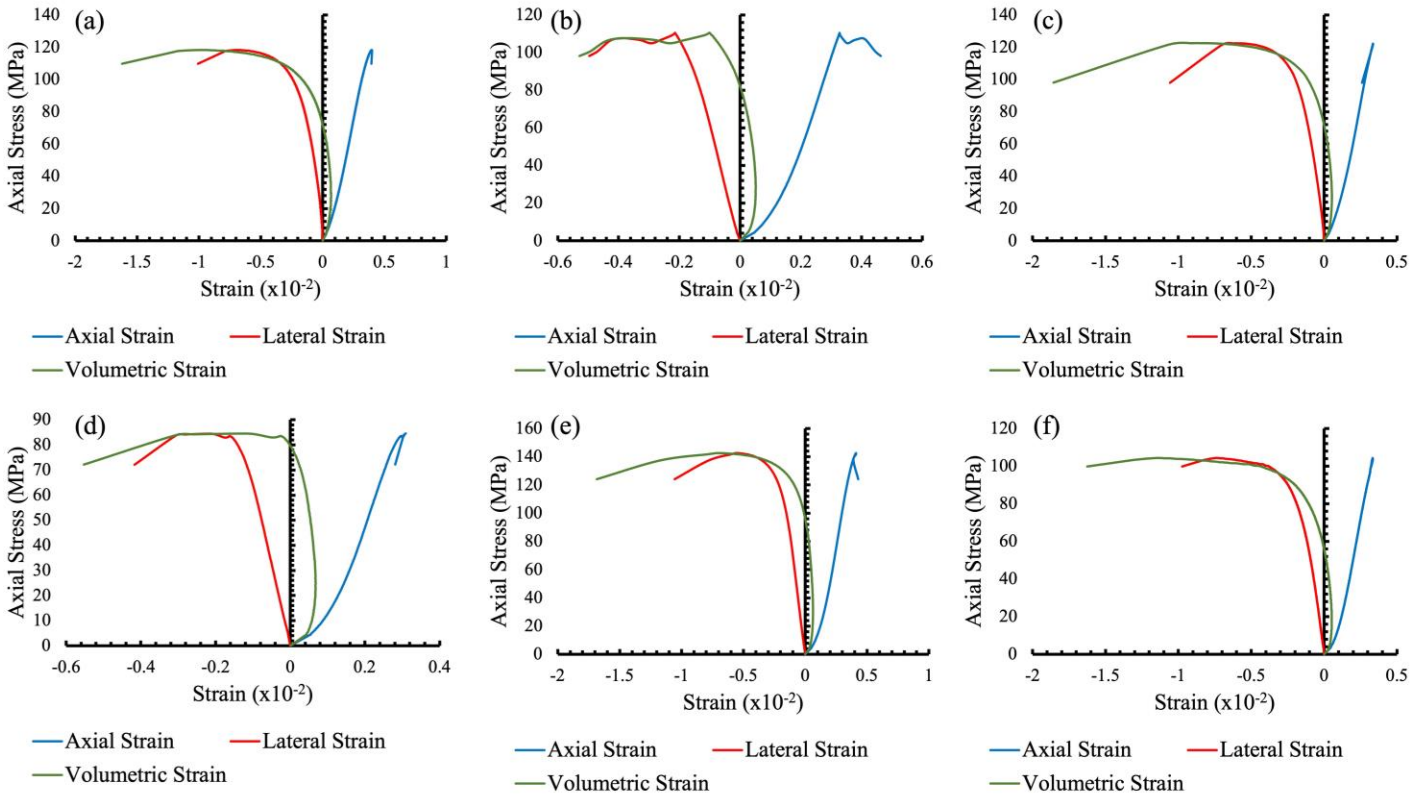

Figure 11. Stress-strain curves of (a) M1; (b) M2; (c) M3; (d) M4; (e) M5; (f) M6.

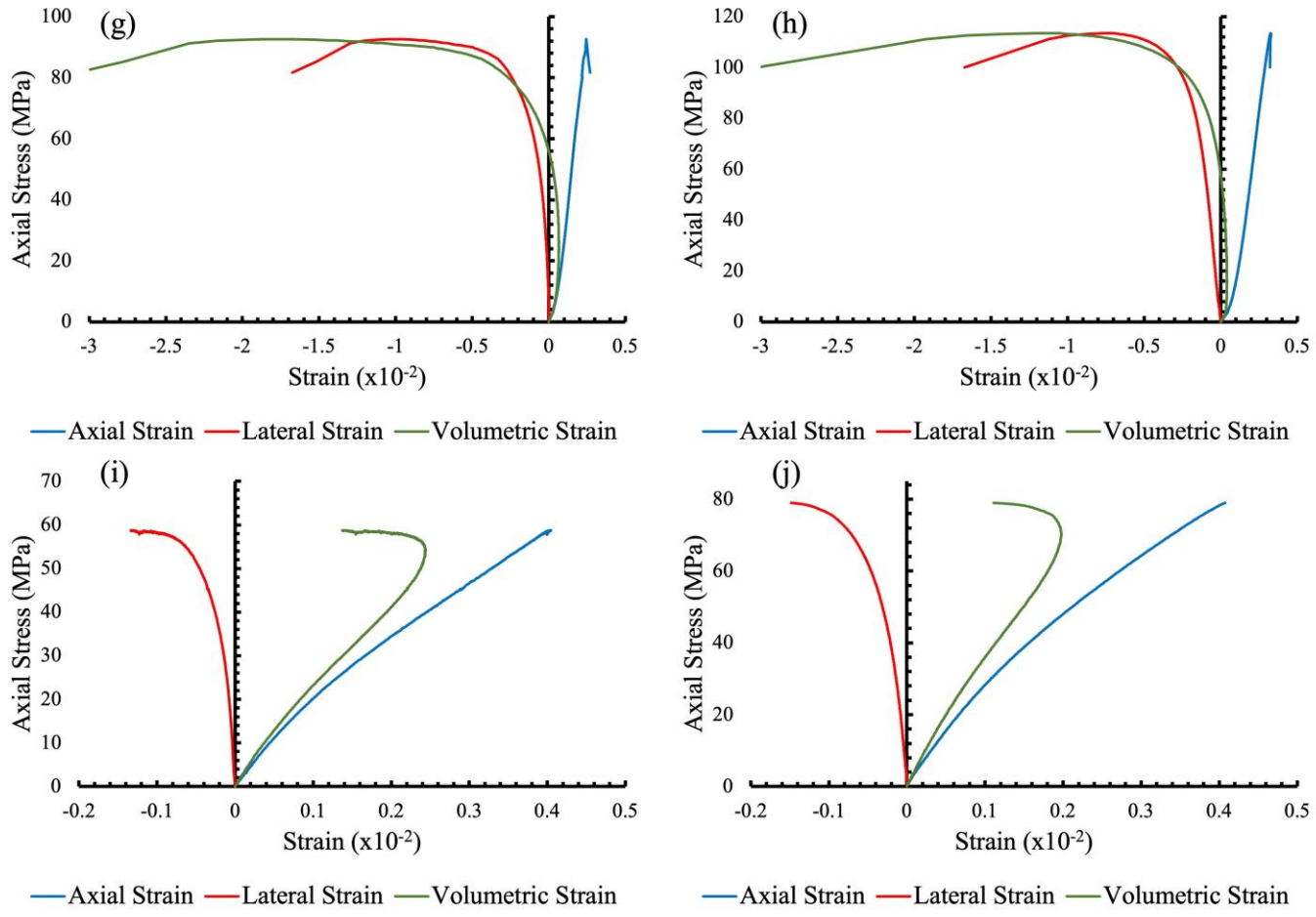

Figure 11. (continued) (g) M7; (h) M8; (i) B1; (j) B2.

References

1. Brace WF, Paulding BW, Scholz C. Dilatancy in the fracture of crystalline rocks. Journal of Geophysical Research. 1966; 71(16): 3939-3953. Doi：https://doi.org/10.1029/JZ071i016p03939
2. Bieniawski ZT. Mechanism of brittle fracture of rock, part I – theory of the fracture process. International Journal of Rock Mechanics and Mining Sciences & Geomechanics Abstracts. 1967; 4(4): 395-404. Doi：https://doi.org/10.1016/0148-9062(67)90030-7
3. Lajtai EZ. Brittle fracture in compression. International Journal of Fracture. 1974; 10(4): 525-536. Doi：https://doi.org/10.1007/BF00155255
4. Stacey TR. A simple extension strain criterion for fracture of brittle rock. International Journal of Rock Mechanics and Mining Sciences & Geomechanics Abstracts. 1981; 18(6): 469-474. Doi：https://doi.org/10.1016/0148-9062(81)90511-8
5. Martin CD, Chandler NA. The progressive fracture of Lac du Bonnet granite. International Journal of Rock Mechanics and Mining Sciences & Geomechanics Abstracts. 1994; 31(8): 643-659. Doi：https://doi.org/10.1016/0148-9062(94)90005-1
6. Eberhardt E, Stead D, Stimpson B, Read R. Identifying crack initiation and propagation thresholds in brittle rocks. Canadian Geotechnical Journal. 1998; 35(2): 222-233. Doi：https://doi.org/10.1139/t97-091
7. Diederichs MS. The 2003 Canadian Geotechnical Colloquium: mechanistic interpretation and practical application of damage and spalling prediction criteria for deep tunnelling. Canadian Geotechnical Journal. 2007; 44(9): 1082-1116. Doi：https://doi.org/10.1139/T07-033
8. Nicksiar M, Martin CD. Evaluation of methods for determining crack initiation in compression tests on low-porosity rocks. Rock Mechanics and Rock Engineering. 2012; 45: 607-617. Doi：https://doi.org/10.1007/s00603-012-0221-6
9. Zhao XG, Cai M, Wang J, Ma LK. Damage stress and acoustic emission characteristics of Beishan granite. International Journal of Rock Mechanics and Mining Sciences. 2013; 64: 258-269. Doi：http://dx.doi.org/10.1016/j.ijrmms.2013.09.003
10. Zhao XG, Cai M, Wang J, Li PF, Ma LK. Objective determination of crack initiation stress of brittle rocks under compression using AE measurement. Rock Mechanics and Rock Engineering. 2015; 48: 2473-2484. Doi：https://doi.org/10.1007/s00603-014-0703-9
11. Wen T, Tang HM, Ma JW, Wang YK. Evaluation of methods for determining crack initiation stress under compression. Engineering Geology. 2018; 235: 81-97. Doi：https://doi.org/10.1016/j.enggeo.2018.01.018
12. Tang MH, Wang GB, Chen SW, Yang CH. An objective crack initiation stress identification method for brittle rock under compression using a reference line. Rock Mechanics and Rock Engineering. 2021; 54: 4283-4298. Doi：https://doi.org/10.1007/s00603-021-02479-y
13. Wen D, Wang X, Ding H, Fu Z. Estimation of Crack Initiation Stress Based on Axial Crack Strain Expansion Rate. Rock Mechanics and Rock Engineering. 2023; 56: 1025-1041. Doi：https://doi.org/10.1007/s00603-022-03113-1
14. Li H, Zhong R, Pel L, Smeulders D, You Z. A New Volumetric Strain-Based Method for Determining the Crack Initiation Threshold for Rocks Under Compression. Rock Mechanics and Rock Engineering. 2024; 57: 1329-1351. Doi：https://doi.org/10.1007/s00603-023-03619-2
15. Fairhurst C, Cook NGW. The phenomenon of rock splitting parallel to the direction of maximum compression in the neighborhood of a surface. Proceedings of the 1st congress of the international society of rock mechanics, September 25 – October 1, 1966, Lisbon, Portugal, pp. 563-577.
16. Hoek E, Brown ET. Underground excavations in rock. The Institution of Mining and Metallurgy, London.
17. Martin CD, Kaiser PK, McCreath DR. Hoek-Brown parameters for predicting the depth of brittle failure around tunnels. Canadian Geotechnical Journal. 1999; 36(1): 136-151. Doi：https://doi.org/10.1139/t98-072
18. Rojat F, Labiouse V, Kaiser PK, Descoeudres F. Brittle rock failure in Steg Lateral Adit of the Lötschberg Base Tunnel. Rock Mechanics and Rock Engineering. 2009; 42: 341-359. Doi：https://doi.org/10.1007/s00603-008-0015-z
19. Martin CD, Christiansson R. Estimating the potential for spalling around a deep nuclear waste repository in crystalline rock. International Journal of Rock Mechanics and Mining Sciences. 2009; 46(2): 219-228. Doi：https://doi.org/10.1016/j.ijrmms.2008.03.001
20. Andersson C, Martin CD, Stille H. The Äspö pillar stability experiment: part II – rock mass response to coupled excavation-induced and thermal-induced stresses. International Journal of Rock Mechanics and Mining Sciences. 2009; 46(5): 865-878. Doi：https://doi.org/10.1016/j.ijrmms.2009.03.002
21. ISRM. Suggested methods for determining the uniaxial compressive strength and deformability of rock materials: Part 1. Suggested method for determining deformability of rock material in uniaxial compression. International Journal of Rock Mechanics and Mining Sciences & Geomechanics Abstracts. 1979; 16(2): 138-140. Doi：https://doi.org/10.1016/0148-9062(79)91451-7
22. Choquette PW, Pray LC. Geologic Nomenclature and Classification of Porosity in Sedimentary Carbonates. AAPG Bulletin. 1970; 54(2): 207-250. Doi：https://doi.org/10.1306/5D25C98B-16C1-11D7-8645000102C1865D
23. Al-Harthi AA, Al-Amri RM, Shehata WM. The porosity and engineering properties of vesicular basalt in Saudi Arabia. Engineering Geology. 1999; 54(3-4): 313-320. Doi：https://doi.org/10.1016/S0013-7952(99)00050-2
24. Zhang Z, Liang Z, Tang C, Kishida K. A Comparative Study of Current Methods for Determining Stress Thresholds of Rock Subjected to Compression. Rock Mechanics and Rock Engineering. 2023; 56: 7795-7818. Doi：https://doi.org/10.1007/s00603-023-03480-3
25. Griffith AA. The phenomenon of rupture and flow in solids. Philosophical Transactions of the Royal Society London. 1921; 221(582-593): 163-198. Doi: https://doi.org/10.1098/rsta.1921.0006
26. Griffith AA. The Theory of Rupture. Proceedings of the 1st International Congress on Applied Mechanics, Delft, Netherlands. 1924; 55-63.